

Tuning magnetic relaxation by oblique deposition

I. Barsukov,^{1,*} P. Landeros,² R. Meckenstock,¹ J. Lindner,^{1,3} D. Spoddig,¹ Zi-An Li,¹ B. Krumme,¹ H. Wende,¹ D. L. Mills,³ and M. Farle¹

¹Fakultät für Physik and Center for Nanointegration Duisburg-Essen (CeNIDE), Universität Duisburg-Essen, D-47048 Duisburg, Germany

²Departamento de Física, Universidad Técnica Federico Santa María, Avenida España 1680, 2390123 Valparaíso, Chile

³Department of Physics and Astronomy, University of California, Irvine, California 92697, USA

(Received 21 December 2011; published 19 January 2012)

Oblique deposition conditions of Si were used to create a periodic compositional defect matrix in Fe₃Si/MgO(001) thin films. The modified growth conditions provoke shadow effects, which lead to a two-magnon scattering channel with twofold symmetry in the film plane. Its axis is controlled by the sample orientation with respect to the Si evaporator. Angular-dependent ferromagnetic resonance data reveal an enhanced magnetic-relaxation rate induced by the dipolar interactions originating from these artificially created defect structures, while magnetic anisotropy is shown to be influenced negligibly. Experimental results agree well with the developed theoretical approach allowing one to distinguish different relaxation channels.

DOI: 10.1103/PhysRevB.85.014420

PACS number(s): 76.60.Es, 75.70.Ak, 75.40.Gb, 76.50.+g

I. INTRODUCTION

The control of spin relaxation is essential for spintronic and spin-torque applications, since the relaxation rate determines the speed at which the magnetization can be reversed. The ability to tailor magnetic relaxation offers opportunities to adjust the stability of magnetization under the influence of rf fields and to tune the critical current for magnetic reversal in spin-torque devices.¹ The spin relaxation is usually discussed in terms of intrinsic and extrinsic processes. The intrinsic ones are referred to as Gilbert damping that can be adjusted by changing the spin-orbit coupling (e.g., by modifying the ferromagnetic material using nonmagnetic dopants).² In principle, the Gilbert damping is anisotropic due to the spin-orbit interaction and has to be treated as a tensorial quantity.³ However, in 3d-based metallic ferromagnets, this anisotropy has been shown to average out.⁴ Consequently, the Gilbert parameter acts as an adjustable, *isotropic* contribution to the overall relaxation. To tailor the overall relaxation with respect to relaxation intensity *and* anisotropic behavior (i.e., preferential directions), extrinsic processes need to be considered. In thin films, the latter are dominated by the two-magnon scattering processes.⁵ Here, the uniform magnons with wave vector $k = 0$ and energy $\hbar\omega$ can be scattered by an effective scattering field into degenerate final-state magnons having the same energy $\hbar\omega$, but a nonzero wave vector $k \neq 0$. This process opens up an additional relaxation channel for the ferromagnetic spin system. It has been shown that the effective scattering field can be created by magnetic roughness⁶ or by defects at film interfaces.⁷⁻¹¹ For spin-torque applications, sharp, epitaxial interfaces are usually essential. Therefore, a method of tailoring the two-magnon process by modifying the film volume, leaving the interfaces intact, is a great advantage.

In this paper, we use oblique angle deposition of Si to incorporate defects within the volume of Fe₃Si/MgO(001) epitaxial thin films. The effective scattering field, which results directly from the defect matrix, induces a two-magnon scattering channel with twofold symmetry, whose preferential direction can be chosen by the deposition angle during film growth and whose scattering rate $\Gamma \sim 0.2$ GHz is comparable

to the Gilbert damping in the X band. This two-magnon scattering process is likely to be of fundamental interest in the framework of tailoring spin relaxation for applications (e.g., in spin valves) and can be well described by the theory presented below.

The Fe₃Si alloy is a promising material for spintronics and spin-torque applications due to its high spin polarization (43% at $T = 0$ K)¹² and small Gilbert parameter, $G \sim 0.05$ GHz.¹³ In epitaxial Fe₃Si/MgO(001) thin films grown by molecular beam epitaxy (MBE), two-magnon scattering processes are natively present. In the X band, their intensity is of the same order of magnitude as the Gilbert damping. In these films, the two-magnon scattering exhibits fourfold symmetry in the film plane with its maxima parallel to the $\langle 100 \rangle_{\text{Fe}_3\text{Si}}$ principal crystallographic directions. Its origin has been identified as resulting from crystalline defects of the alloy.¹³ The mechanism that leads to two-magnon scattering, however, has not been explained so far.¹¹ In this paper, we have extended the theory of Arias and Mills⁷ to describe the in-plane dependence of the scattering process that in turn is reflected by anisotropic angular dependence of the linewidth of the ferromagnetic resonance (FMR) signal. We use the extension to clearly extract and quantitatively fit the fourfold two-magnon contribution. We will show that the additional twofold contribution can be controlled by creating chemical disorder with a symmetry axis along any given in-plane direction and thus independently of the fourfold contribution.

II. THEORY

Following Arias and Mills formalism^{7,14,15} based on the linear response theory, it is possible to construct a generalized dynamic susceptibility, whose denominator includes information about the FMR *frequency* and FMR *linewidth*. This theory includes intrinsic and extrinsic damping mechanisms, and the FMR linewidth associated with both damping mechanisms can be written as

$$\Delta B = \Delta B_{\text{intr}} + \Delta B_{\text{extr}} = \frac{\alpha\omega}{\gamma\Psi} + \frac{\Gamma}{\gamma\Psi}. \quad (1)$$

Note that to obtain the peak-to-peak linewidth, we need to multiply ΔB by a factor $2/\sqrt{3}$. In the above equation, α is the dimensionless Gilbert damping parameter (intrinsic damping), Γ is the two-magnon scattering rate (extrinsic damping), γ is the spectroscopic splitting factor including the g factor via $\gamma = \mu_B g/\hbar$, ω is the microwave frequency, and Ψ is the *dragging* function generally given by

$$\Psi = \frac{1}{\gamma^2[W_x + W_y]} \frac{d(\omega_{\text{FMR}}^2)}{dB_{\text{ext}}}. \quad (2)$$

The dragging of the magnetization has to be taken into account due to the fact that in the FMR experiment, the microwave frequency is fixed as the eigenfrequency of the microwave cavity, while the external magnetic field B_{ext} is swept, and the vectors of the magnetization and external magnetic field may be nonparallel. In our case, the resonance frequency obeys the relation $\omega_{\text{FMR}}^2 = \gamma^2 W_x W_y$, and, therefore, the dragging function becomes

$$\Psi = \frac{1}{W_x + W_y} \left(\frac{dW_x}{dB_{\text{ext}}} W_y + \frac{dW_y}{dB_{\text{ext}}} W_x \right), \quad (3)$$

where W_x and W_y are the *stiffness fields* that are for the system considered in this paper:

$$W_x = B_{\text{ext}} \cos(\phi - \phi_B) + B_{\text{uniax}} \cos[2(\phi_{\text{uniax}} - \phi)] + B_{\text{cryst}} \cos[4(\phi_{(100)} - \phi)] \quad (4)$$

and

$$W_y = B_{\text{ext}} \cos(\phi - \phi_B) + B_{\perp} + B_{\text{uniax}} \cos^2(\phi_{\text{uniax}} - \phi) + B_{\text{cryst}} \{\cos[4(\phi_{(100)} - \phi)] + 3\}/4. \quad (5)$$

Here B_{uniax} , B_{cryst} , and B_{\perp} are the uniaxial, the magnetocrystalline, and the effective perpendicular anisotropy fields; the latter, sometimes referred to as $B_{\perp} = \mu_0 M_{\text{eff}}$, represents the shape anisotropy (depending on the saturation magnetization via $\mu_0 M_s$) and out-of-plane anisotropy fields (including the surface anisotropy contribution). $\phi_{(100)}$ is the $\langle 100 \rangle$ axis of Fe_3Si , and ϕ_{uniax} is the angle of hard axis of the uniaxial anisotropy in the film plane. ϕ represents the direction of the magnetization. Since in Fe_3Si the in-plane anisotropy is relatively weak, this direction corresponds to the direction of the external magnetic field, $\phi \approx \phi_B$, to a good approximation.

While, in Fe_3Si , the Gilbert damping is isotropic,¹³ the extrinsic two-magnon scattering process is anisotropic in the film plane. The Arias-Mills theory^{7,14,15} allows one to include these *extrinsic* relaxation processes, represented by Γ in Eq. (1), which depend mainly on the specific form of the array of defects in the film, since the latter mediates the scattering of the uniform magnons into the nonuniform final-state magnons. In this paper, we consider two kinds of defects structures: (i) The first is an array of crystalline defects building rectangular structures that are randomly distributed over the film plane and oriented parallel to the in-plane principal crystallographic axes of Fe_3Si ($\langle 100 \rangle$ and $\langle 110 \rangle$). To model the scattering field arising from these defects, the theory from Refs. 7 and 14 that considers rectangular ‘‘bump’’ defects is employed and further developed. (ii) The second type is an array of defects in the film plane in the form of periodic stripes with slightly different saturation magnetization [Fig. 1(a)], causing dipolar fields among the defects to induce a two-magnon scattering channel.

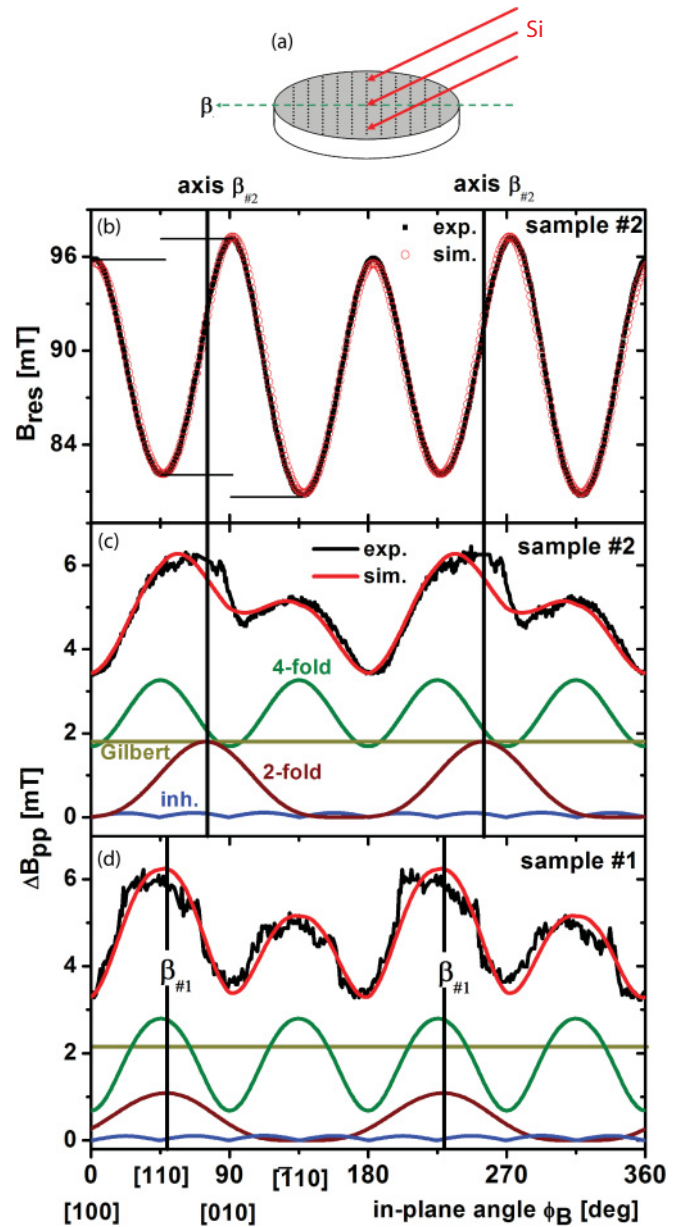


FIG. 1. (Color online) (a) Sketch of the film deposition geometry. Oblique deposition of Si causes striplike defects with the symmetry axis perpendicular to the projection of the Si flow β . (b)–(d) 40 nm $\text{Fe}_3\text{Si}/\text{MgO}(001)$ FMR data at 9.3 GHz. (b) In-plane angular dependence of FMR resonance fields, revealing the fourfold crystalline anisotropy K_4^{\parallel} and the small uniaxial anisotropy K_2^{\parallel} . (c) FMR linewidth: The native fourfold contribution Γ_{fourfold} caused by crystalline defects is superimposed by the twofold contribution Γ_{twofold} . The maximum of the latter one is parallel to the hard axis of the uniaxial anisotropy and corresponds to the in-plane projection of the Si flow: $\phi_{\text{twofold}} = \phi_{\text{uniax}} = \beta$. (d) Linewidth of the sample no. 1, for which the axis β was set close to the $\langle 100 \rangle$ direction.

To model such dipolar fields, a striplike stepped modulation of the film surface is taken as the basis of the calculations. We consider the dipolar fields calculated within this picture to be comparable to the fields emerging from defects in the form of variation of the chemical composition constrained to the film volume.

We will show that the two-magnon scattering channel originating from these defect structures differs substantially when the applied field is rotated within the film plane. The derivation of the contributions to the linewidth of these relaxation channels is too lengthy to detail here and will be presented in a forthcoming paper.¹⁶

For the first kind of defect structure, the linewidth associated to the array of randomly located defects of rectangular shape (fourfold symmetry) can be obtained by calculating the energy difference attributed to the defect array with respect to the spin-wave Hamiltonian of the perfect film. We obtain the scattering rate of the two-magnon scattering^{7,14,15} as

$$\Gamma_{\text{fourfold}} = \frac{8\gamma b^2 B_{\text{def}}^2 p a c (g_x W_y + g_y W_x)^2 \phi_c}{\pi D (W_x + W_y)^2}, \quad (6)$$

$$g_x = (a^{-1} - c^{-1}) \cos[2(\zeta - \phi)], \quad (7)$$

$$g_y = (a^{-1} - c^{-1}) \cos^2(\zeta - \phi) - a^{-1}, \quad (8)$$

$$\phi_c = \arcsin \sqrt{W_x/W_y}. \quad (9)$$

Here, p is the fraction of the surface covered by defects with effective lateral dimensions a and c .^{7,14,15} D is the exchange stiffness, which has been evaluated from spin-wave resonance measurements at high frequencies, b is the effective height of the defects, and B_{def} is the interface anisotropy field of the defects. This mechanism results in an in-plane angular dependence of the relaxation channel with a fourfold symmetry. Since there are two sets of rectangular defects, oriented along $\langle 100 \rangle$ and $\langle 110 \rangle$ (these axes are denoted as ζ), respectively, two relaxation channels, both with fourfold symmetry but rotated by 45° with respect to each other, occur. Their superposition reveals a fourfold symmetry again. The overall two-magnon scattering rate is parameterized by the maximal scattering rate of these relaxation channels, termed $\Gamma_{(100)}^{\text{max}}$ and $\Gamma_{(110)}^{\text{max}}$.

For the second kind of defect structure, the theoretical analysis of the linewidth associated to the relaxation channel induced by the dipolar fields among stripelike defects is rather extensive and will be presented elsewhere.¹⁶ Basically, we write the magnetization of the stripe defects in the following way:

$$M_z(z') = M_s \cos(\phi - \phi_{\text{twofold}}) \sum_{n=-\infty}^{\infty} \Theta\left(z' - \left\{na_0 - \frac{w}{2}\right\}\right) \times \Theta\left(\left\{na_0 + \frac{w}{2}\right\} - z'\right), \quad (10)$$

where z' is the normal to the stripes within the film plane, and ϕ_{twofold} denotes the angle of this axis, therefore, $(\phi - \phi_{\text{twofold}})$ is the in-plane angle between the magnetization and z' . Also, a_0 is the periodicity, w is the width, and h is the height of the stripes, and $\Theta(x)$ represents the Heaviside θ function, which is equal to 0 for $x < 0$ and 1 for $x > 0$. The next step is to calculate the dipole field produced by the above magnetization, which reads

$$h_z(z') = -4hg_0 M_s \cos(\phi - \phi_{\text{twofold}}) \times \sum_{n=1}^{\infty} \sin\left(\frac{ng_0 w}{2}\right) \cos(ng_0 z') e^{-ng_0 |d-y|}, \quad (11)$$

where $g_0 = 2\pi/a_0$, d is the film thickness, and y is the coordinate normal to the film. Now one can obtain the dipole energy associated to the stripes and write down the matrix elements of the two-magnon scattering matrix,^{7,14} that is

$$V_{xx}(\mathbf{k}', \mathbf{k}) = -hg_0 \cos^2(\phi - \phi_{\text{twofold}}) \sum_{n=1}^{\infty} \sin\left(\frac{ng_0 w}{2}\right) \times \frac{1 - e^{-ng_0 d}}{ng_0 d} (\delta_{\mathbf{k}', \mathbf{k} + \mathbf{g}_n} + \delta_{\mathbf{k}', \mathbf{k} - \mathbf{g}_n}), \quad (12)$$

where $\mathbf{g}_n = ng_0 \hat{\mathbf{z}}$, and \mathbf{k} is a wave vector confined in the plane of the film. The remaining matrix elements are $V_{yy}(\mathbf{k}', \mathbf{k}) = V_{xx}(\mathbf{k}', \mathbf{k})$, and $V_{xy}(\mathbf{k}', \mathbf{k}) = V_{yx}(\mathbf{k}', \mathbf{k}) = 0$. The next task is to work out the elements of the proper self-energy. We begin with Eqs. (36) and (37) of Ref. 7 and then generate an effective Dyson-like equation to the second order in $V_{\alpha\beta}$. This process allows us to obtain a complete set of response functions from which we can extract information about the two-magnon linewidth and frequency shift with origin in the stray fields produced at the edges of the stripes. As explained in detail in a forthcoming paper,¹⁶ the imaginary part of the response function S_{xx} is given by

$$S_{xx}^{\text{Im}} = \gamma M_s \frac{\gamma W_y (\Lambda^0 + F^{\text{Im}}) - \alpha \omega (\omega_{\text{FMR}}^2 - \omega^2)}{(\omega_{\text{FMR}}^2 - \omega^2)^2 + (\Lambda^0 + F^{\text{Im}})^2}, \quad (13)$$

where $\Lambda^0 = \alpha \omega \gamma (W_x + W_y)$ represents the Gilbert damping contribution, and

$$F^{\text{Im}} = 2g_0^2 h^2 \gamma^2 M_s^2 \cos^4(\phi - \phi_{\text{twofold}}) \times \sum_{n=1}^{\infty} \sin^2\left(\frac{ng_0 w}{2}\right) \left(\frac{1 - e^{-ng_0 d}}{ng_0 d}\right)^2 \times \frac{[\gamma^2 (W_x^2 + W_y^2) + 2\omega^2] \Lambda(\mathbf{g}_n) - 2[\omega^2(\mathbf{g}_n) - \omega^2] \Lambda^0}{[\omega^2(\mathbf{g}_n) - \omega^2]^2 + \Lambda(\mathbf{g}_n)^2}$$

is the contribution from the stripe defects. Here,

$$\Lambda(\mathbf{k}) = \alpha \omega \gamma \left[W_x + W_y - 4\pi M_s \left(1 - \frac{1 - e^{-kd}}{kd}\right) \cos^2 \phi_{\mathbf{k}} + 2Dk^2 \right], \quad (14)$$

where $\phi_{\mathbf{k}}$ is the angle between the wave vector and the magnetization. Finally, the two-magnon scattering rate activated by the dipolar fields emerging from stripelike defects is given by

$$\Gamma_{\text{twofold}} = \frac{F^{\text{Im}}}{\gamma (W_x + W_y)} \approx \Gamma_{\text{twofold}}^{\text{max}} \cos^4(\phi - \phi_{\text{twofold}}), \quad (15)$$

since the function F^{Im} defined above is approximately proportional to $\cos^4(\phi - \phi_{\text{twofold}})$. In the following, the scattering rate is parameterized by its intensity $\Gamma_{\text{twofold}}^{\text{max}}$ and the axis of maximal scattering rate ϕ_{twofold} .

III. EXPERIMENT

In order to open up an additional spin-relaxation channel, we modified the growth conditions by tilting the Si evaporator in the MBE chamber, whereas the orientation of the Fe evaporator was left unchanged. Thus, the Si flow enters the substrate plane under an oblique angle of approximately 15° with respect

to the film normal. The projection of the Si flow on the film plane is referred to as axis β in the following. Such growth conditions are known to provoke so-called shadow effects.^{17–21} Although Fe₃Si grows on MgO(001) without forming distinct islands from a film thickness of 7 ML,²² the film surface still exhibits roughness on the atomic scale during film growth, which acts as a barrier for the oblique deposition of Si. This in turn leads to a slight, spatial variation of Si concentration, forming a defect matrix of varying chemical composition, which has a pseudorandom distribution but nevertheless a twofold, stripelike symmetry. Despite the modified growth process, our structural investigation by means of conversion electron Mössbauer spectroscopy (CEMS) revealed no change of the prevalence of the D0₃ structure—in particular, the short-range ordering parameters are similar to those of the films grown by nonoblique deposition. Several Fe₃Si/MgO(001) films were grown as described in Ref. 13, and the in-plane direction of the Si flow was controlled.

Furthermore, to evaluate the structural consequences of the oblique deposition, we conducted investigations on the sample morphology. The topography of the MgO(001) substrate prior to deposition, as well as of the film itself, was evaluated by means of atomic force microscopy (AFM), which did not show any anisotropy of these interfaces. By means of a focused ion beam (FIB), cross-section lamellae parallel and perpendicular to the projection of the Si flow were produced. They were further studied by high-resolution transmission electron microscopy (HRTEM) and energy-dispersive x-ray spectroscopy (EDX). The results of these measurements are discussed below in relation to the magnetic investigations.

IV. RESULTS AND DISCUSSION

Using the saturation magnetization $M_s = 0.96(8) \times 10^6$ A/m measured by SQUID magnetometry,¹³ the in-plane angular dependence of the FMR fields, measured at 9.3 GHz and shown in Fig. 1(b), has been fitted.²³ The effective perpendicular anisotropy field is $B_{\perp} \approx 1$ T. The in-plane magnetocrystalline anisotropy constant is found to be $K_4^{\parallel} \approx (3.3\text{--}4.3) \times 10^3$ J/m³. The in-plane *uniaxial* anisotropy constant is small [compare the twofold and fourfold contributions in Fig. 1(b)] and amounts to $K_2^{\parallel} \approx (0.1\text{--}0.5) \times 10^3$ J/m³.

Except for this small uniaxial anisotropy, a comparison with anisotropy values of the samples grown by nonoblique deposition reveals that the modified growth conditions do not considerably change the static magnetic parameters. However, there is a correlation of the in-plane uniaxial anisotropy K_2^{\parallel} and the sample preparation. The hard axis ϕ_{uniax} of K_2^{\parallel} is aligned parallel to the in-plane projection of the Si flow β . Indeed, stripelike defects caused by the shadow effect are known to induce such magnetic anisotropy in thin films by means of the *dipolar interactions* among the defects.^{21,24} The low value of K_2^{\parallel} suggests a *low density* of these defects.

The FMR linewidth allows one to access the relaxation processes in the sample. As shown in Fig. 1(c), the in-plane angular dependence exhibits a behavior remarkably different from that of a regular film grown with a nontilted Si evaporator shown in Ref. 13. While it has the same fourfold symmetry typical for Fe₃Si/MgO(001) films, it also is superimposed by

an additional twofold contribution. The latter is significantly large, being of the same order of magnitude as the fourfold contribution and the Gilbert contribution.

For a quantitative evaluation of the relaxation processes, several contributions to the FMR linewidth must be considered.^{5,13} First, any line broadening due to the finite conductivity, exchange-conductivity effect, and nonanalytical line broadening caused by surface anisotropy has been calculated using the theory of Frait and Fraitová²⁵ and found to be negligible.¹³ Therefore, the linewidth can be referred to as

$$\Delta B = \Delta B_{\text{inh}} + \Delta B_{\text{intr}} + \Delta B_{\text{extr}}. \quad (16)$$

While ΔB_{intr} and ΔB_{extr} have been introduced in the theoretical section [Eq. (1)], the inhomogeneous line broadening ΔB_{inh} needs to be accounted for due to the spatial variation of internal fields in the real samples that leads to a superposition of slightly shifted absorption peaks. In Fe₃Si/MgO(001) epitaxial films, this contribution is dominated by a slight in-plane misalignment of the crystallites' axes in the film plane. As explained in Ref. 13, this contribution is proportional to the first derivative of the FMR fields with respect to the in-plane angle $\partial B_{\text{res}}/\partial \phi_B$ and to an effective misalignment of the crystallites $\Delta\phi_{\text{inh}}$. This contribution is small ($<0.5 \times 10^{-3}$ T) and can be separated from other contributions due to its specific angular dependence. The values of $\Delta\phi_{\text{inh}} < 0.5^\circ$ lie in the same range as those of the samples grown by nonoblique deposition. We conclude that the inhomogeneity of the sample is not affected by the modified growth conditions with the oblique deposition angle used here.

Due to the anisotropy fields, the direction of magnetization and of the external field may differ. This causes dragging effects, which result in an increase of the linewidth. To account for these effects, a factor of $1/\Psi$ ¹⁵ must be applied to the intrinsic and extrinsic damping contributions [see Eq. (1)]. The dragging function Ψ according to Eq. (3) has been calculated; it is very close to 1 for the samples discussed in this paper, so that the contribution of the dragging effects to the linewidth is smaller than 1% and therefore neglected in what follows.

As discussed above, the contribution from the Gilbert damping $\alpha\omega/\gamma$ is isotropic.⁴ In particular for Fe₃Si/MgO(001) thin films, this isotropy has been proven experimentally.¹³ To fit the experimental linewidth, we use the contributions of the inhomogeneous line broadening, the Gilbert damping, and both two-magnon relaxation channels Γ_{fourfold} along $\langle 100 \rangle$ and $\langle 110 \rangle$ and Γ_{twofold} described in the theoretical section. As shown in Figs. 1(c) and 1(d) for two different samples, the linewidth can be fitted well. The in-plane angular dependences of the different contributions to the linewidth are characteristic and can therefore be separated. To verify the results, however, additional in-plane angle-dependent FMR measurements at higher frequencies have been performed, and the data were fitted with the same set of parameters (similar to the procedure described in Ref. 13). We obtain the parameters $\Gamma_{\langle 100 \rangle}^{\text{max}}$, $\Gamma_{\langle 110 \rangle}^{\text{max}}$, $\Gamma_{\text{twofold}}^{\text{max}}$, and ϕ_{twofold} , which are collected in Table I. We find no significant change of the Gilbert parameter due to the modified growth conditions, which is in accordance with the fact that the short-range order measured by CEMS is not affected by the oblique deposition.

TABLE I. Static and dynamic magnetic parameters (at X band) of Fe₃Si/MgO(001) prepared under different growth conditions. The error bar amounts to <10% of the anisotropy constants, ~30% of Γ_{ζ}^{\max} , <10% of $\Gamma_{\text{twofold}}^{\max}$, and <5° of ϕ_{twofold} .

Sample, Si deposition, and film thickness	K_4^{\parallel} (10^3 J/m ³)	K_2^{\parallel} (10^3 J/m ³)	$\Gamma_{(100)}^{\max}$ (10^7 Hz)	$\Gamma_{(110)}^{\max}$ (10^7 Hz)	$\Gamma_{\text{twofold}}^{\max}$ (10^7 Hz)	ϕ_{twofold} (deg)
No. 1 oblique, 40 nm	4.0	0.2	51	13	20	49
No. 2 oblique, 40 nm	3.8	0.5	58	30	33	74
No. 3 oblique, 40 nm, not annealed	2.7	0.25	269	95	33	74
No. 4 oblique, 10 nm	4.3	<0.1	52	14	10	48
No. 5 normal, 40 nm (from Ref. 13)	3.3		53	26		

As shown in Table I, the modified growth conditions also do not affect the fourfold two-magnon scattering process Γ_{fourfold} . Its intensity is comparable with results presented in Ref. 13. A comparison of the results of samples no. 1 and no. 3 (see Table I) reveals that despite the modified growth, the Γ_{fourfold} intensity—correlating to the number of crystalline defects—can be decreased by means of sample annealing.

Resorting to the elementary mechanisms provoking two-magnon scattering in the framework of the theory of Arias and Mills,⁷ the *twofold* in-plane scattering channel can only be achieved by means of *dipolar* interactions among the scattering centers. Such interactions are likely to be present due to the shadow effects in films prepared by oblique deposition. The uniaxial anisotropy K_2^{\parallel} supports this assumption due to its dipolar origin.²¹ According to previous works on the structural characterization of shadow effects,^{20,21} a periodic array of stripe defects, such that two-magnon scattering is activated by dipole fields with origin on the stripe edges,¹⁶ has been considered. The axis of maximal scattering intensity is parallel to the hard axis of the uniaxial anisotropy, $\phi_{\text{twofold}} = \phi_{\text{uniax}}$, and, in turn, is parallel to the in-plane projection of the Si flow β , which shows a good agreement of theory and experiment.

The *lateral* scanning electron microscopy (SEM)-EDX studies on the large length scale reveal that the relative variation of chemical composition cannot be larger than 5%. In contrast to the fact that annealing heals the crystalline defects and reduces the fourfold two-magnon scattering Γ_{fourfold} , it seems not to affect the twofold two-magnon scattering Γ_{twofold} (compare sample no. 3 with no. 1 or no. 2 in Table I). The distance between the stripelike defects has to be much larger than the interdiffusion length; for the latter, we can assume a value of at least several tens of superlattices (0.567 nm) of Fe₃Si. Also, the HRTEM and EDX measurements on cross-section lamellae did not show position-dependent variation of the crystalline structure or variation of the chemical composition parallel and perpendicular to the axis β on the length scale of 150 nm. It is remarkable that the low density of stripelike defects causes a negligible uniaxial anisotropy and does not affect other static magnetic parameters, but induces a significantly large

twofold two-magnon scattering. This fact, we conclude, can be of interest for application purposes. The reason must lie in the periodicity of the defects. We calculated the optimal value for averaged distances between the stripes to be on the order of magnitude of a hundred nanometers. Note that a further increase of the deposition angle would lead to stronger shadow effects, which then would be easily detectable, as studies in Refs. 20 and 21 show. However, in this case, several strongly unsolicited effects would appear, such as increased inhomogeneity of the sample, surface roughness, large uniaxial anisotropy, and additional damping contributions.

V. CONCLUSIONS

In conclusion, we show that after explaining the nature of the fourfold two-magnon process emerging from crystalline defects, an additional twofold two-magnon process has been shown to be related to the oblique deposition of Si. We identify the dipolar interaction among a twofold low-density defect matrix to be the mechanism for this scattering channel. Its axis of maximal intensity is not associated with crystallographic directions and can be chosen deliberately by orientation of the sample with respect to the Si evaporator. The scattering channel originates from defects in the film volume. The method of oblique deposition may be applicable to other systems consisting of two elements or more and can become of interest for application insofar as the crystalline quality and the static magnetic parameters are not influenced by the modified growth conditions and, furthermore, the film interfaces are not involved in this procedure.¹⁰

ACKNOWLEDGMENTS

The authors thank U. von Hörsten for preparing the samples, Z. Frait and D. Fraitová for fruitful discussions, and M. Spasova and S. Stienen for their help. Financial support by the DFG, SFB 491 is acknowledged. J.L. thanks the Alexander von Humboldt Foundation for financial support. P.L. acknowledges support from FONDECYT Grant No. 1120618 and CEDENNA Grant No. FB0807.

*igor.barsukov@uni-due.de

¹G. D. Fuchs, N. C. Emley, I. N. Krivorotov, P. M. Braganca, E. M. Ryan, S. I. Kiselev, J. C. Sankey, D. C. Ralph, R. A. Buhrman, and J. A. Katine, *Appl. Phys. Lett.* **85**, 1205 (2004).

²C. Scheck, L. Cheng, I. Barsukov, Z. Frait, and W. E. Bailey, *Phys. Rev. Lett.* **98**, 117601 (2007).

³M. Fähnle and D. Steiauf, *Phys. Rev. B* **73**, 184427 (2006).

⁴J. Seib, D. Steiauf, and M. Fähnle, *Phys. Rev. B* **79**, 092418 (2009).

- ⁵C. W. Haas and H. B. Callen, in *Magnetism, Volume I*, edited by G. T. Rado and H. Suhl (Academic, New York, 1963).
- ⁶B. Hillebrands (private communication).
- ⁷R. Arias and D. L. Mills, *Phys. Rev. B* **60**, 7395 (1999).
- ⁸A. Azevedo, A. B. Oliveira, F. M. de Aguiar, and S. M. Rezende, *Phys. Rev. B* **62**, 5331 (2000).
- ⁹R. D. McMichael, D. J. Twisselmann, J. E. Bonevich, A. P. Chen, and W. F. Egelhoff Jr., *J. Appl. Phys.* **91**, 8647 (2002).
- ¹⁰G. Woltersdorf and B. Heinrich, *Phys. Rev. B* **69**, 184417 (2004).
- ¹¹I. Barsukov, R. Meckenstock, J. Lindner, M. Möller, C. Hassel, O. Posth, M. Farle, and H. Wende, *IEEE Trans. Magn.* **46**, 2252 (2010).
- ¹²K. Zakeri, I. Barsukov, N. K. Utochkina, F. M. Römer, J. Lindner, R. Meckenstock, U. von Hörsten, H. Wende, W. Keune, M. Farle, S. S. Kalarickal, K. Lenz, and Z. Frait, *Phys. Rev. B* **76**, 214421 (2007).
- ¹³Kh. Zakeri, J. Lindner, I. Barsukov, R. Meckenstock, M. Farle, U. von Hörsten, H. Wende, W. Keune, J. Rucker, S. S. Kalarickal, K. Lenz, W. Kuch, K. Baberschke, and Z. Frait, *Phys. Rev. B* **76**, 104416 (2007).
- ¹⁴P. Landeros, R. E. Arias, and D. L. Mills, *Phys. Rev. B* **77**, 214405 (2008).
- ¹⁵J. Lindner, I. Barsukov, C. Raeder, C. Hassel, O. Posth, R. Meckenstock, P. Landeros, and D. L. Mills, *Phys. Rev. B* **80**, 224421 (2009).
- ¹⁶P. Landeros and D. L. Mills (unpublished).
- ¹⁷Y. Hoshi, E. Suzuki, and M. Naoe, *J. Appl. Phys.* **79**, 4945 (1996).
- ¹⁸Hidehiko Harada, Shinji Jomori, Motofumi Suzuki, Kohei Kinoshita, Kaoru Nakajima, and Kenji Kimura, *Thin Solid Films* **515**, 8277 (2007).
- ¹⁹Nguyen N. Phuoc, Feng Xu, and C. K. Ong, *J. Appl. Phys.* **105**, 113926 (2009).
- ²⁰Qing-feng Zhan, Chris Van Haesendonck, Stijn Vandezande, and Kristiaan Temst, *Appl. Phys. Lett.* **94**, 042504 (2009).
- ²¹J. H. Wolfe, R. K. Kawakami, W. L. Ling, Z. Q. Qiu, R. Arias, and D. L. Mills, *J. Magn. Magn. Mater.* **232**, 232 (2001).
- ²²B. Krumme, C. Weis, H. C. Herper, F. Stromberg, C. Antoniak, A. Warland, E. Schuster, P. Srivastava, M. Walterfang, K. Fauth, J. Minár, H. Ebert, P. Entel, W. Keune, and H. Wende, *Phys. Rev. B* **80**, 144403 (2009).
- ²³M. Farle, *Rep. Prog. Phys.* **61**, 755 (1998).
- ²⁴J. L. Bubendorff, S. Zabrocki, G. Garreau, S. Hajjar, R. Jaafar, D. Berling, A. Mehdaoui, C. Pirri, and G. Gewinner, *Europhys. Lett.* **75**, 119 (2006).
- ²⁵Z. Frait and D. Fraitová, in *Spin-Wave Resonance in Metals*, edited by A. S. Borovik-Romanov and S. K. Sinha (Elsevier, Amsterdam, 1998).